A new technique in retrieving Total Electron Content and second-order ionospheric delays in radio occultation experiments using GPS

Panagiotis Vergados* and Spiros D. Pagiatakis
Department of Physics and Astronomy, York University
4700 Keele Street, Toronto, Ontario M3J 1P3, Canada. *vergados@yorku.ca, spiros@yorku.ca

I. Introduction

Radio occultation (RO) is a technique used for probing the Earth's atmosphere since 1995 [*Anthes et al.,* 2008]. Receivers on board Low Earth Orbiters (LEO) record both, the amplitude and phase of the transmitted dual frequency (L_1: f_1=1.57542 GHz; L_2: f_2=1.22760 GHz) Global Positioning System (GPS) signals traversing the Earth's ionosphere and neutral atmosphere, as the GPS satellites set or rise behind the Earth's limb. To remove the ionospheric contribution from the GPS measurements, *Guier and Weiffenbach* [1960] suggested forming the ionosphere-free linear combination between GPS observables. Nevertheless, second- and higher-order ionospheric residuals remain uncorrected, limiting the GPS measurements accuracy. Nowadays, the achieved accuracy in point positioning is at the centimeter-level. However, recent GPS advancements in monitoring plate tectonic motion, crustal deformation and atmospheric sounding require millimeter-level accuracy [*Bos,* 2005]. Hence, the assessment of the impact of the second-order ionospheric effect on GPS applications gained the interest of the scientific community. *Morton et al.* [2009] estimated the second-order ionospheric effect for ground-based receiver positioning within [1, 10] mm. However, on RO measurements and their derived products, there is not any information about the magnitude and impact of the second-order ionospheric effect [*Anthes et al.,* 2008]. This paper introduces an algorithm that determines the second-order ionospheric delay in RO experiments in near-real time. A new technique to estimate STEC free from the second-order ionospheric effect is also introduced, using level-1b data from the Constellation Observing System for Meteorology, Ionosphere and Climate (COSMIC).

II. Methodology

Taking into consideration the second-order ionospheric effect, we can model the ionospheric L_1 and L_2 GPS phase measurements, using the observation equations:

$$(L_1-\rho)\cong-\frac{40.3}{f_1^2}\cdot STEC_1-\frac{K\cdot\langle B_\parallel\rangle_1}{f_1^3}+\lambda_1N_1+b^{GPS,L_1}+b_{LEO,L_1}+mp_{L_1}+\varepsilon_{L_1} \tag{1}$$

$$(L_2-\rho)\cong-\frac{40.3}{f_2^2}\cdot STEC_2-\frac{K\cdot\langle B_\parallel\rangle_2}{f_2^3}+\lambda_2N_2+b^{GPS,L_2}+b_{LEO,L_2}+mp_{L_2}+\varepsilon_{L_2} \tag{2}$$

where ρ is the GPS/LEO line-of-sight (LoS) (m), $STEC_i=\int_{GPS}^{LEO}n_e^{(i)}ds$ is the slant total electron content (TECU) and $\langle B_\parallel\rangle_i=\int_{GPS}^{LEO}B\cos\theta\cdot n_e^{(i)}ds$ is the geomagnetic field (T/m^2) weighted by the electron number density n_e along the propagation path (i=1,2 represents the two GPS frequencies). λ_1, λ_2 (m), N_1, N_2, b^{GPS,L_1}, b^{GPS,L_2}, b_{LEO,L_1}, b_{LEO,L_2}, mp_{L_1}, mp_{L_2}, and ε_{L_1}, ε_{L_2} are the wavelengths, the integer carrier-phase ambiguities, the inter-frequency biases, multipath and noise at L_1, L_2 channels, respectively. CDAAC estimates RO STEC by differencing the L_1 and L_2 GPS observables:

$$STEC=\frac{f_1^2f_2^2}{40.3(f_1^2-f_2^2)}(L_1-L_2) \tag{3}$$

Syndergaard [2002] suggested a different approach in estimating RO STEC by accounting for the ionospheric bending and/or dispersion effects through the following equation:

$$STEC = \frac{f_2^4 L_2 - f_1^4 L_1}{40.3(f_1^2 - f_2^2)} \tag{4}$$

Equations (3) and (4) do not account for the ray path splitting between the L_1 and L_2 signals, disregard second-order ionospheric effects, the L_1 and L_2 carrier-phase ambiguities, local multipath, background ionospheric noise, scintillation effects and receiver clock errors. To improve the STEC estimates at all conditions, we consider the ray path splitting between the L_1 and L_2 GPS signals. Solving Eqs. (1) and (2) for $STEC_1$ and $STEC_2$ and assuming that the geomagnetic field is the same for both paths (because the ray path splitting between the GPS signals is small), we get:

$$STEC_1 = -\frac{(L_1 - \rho)}{40.3} \cdot f_1^2 - \frac{K \cdot \langle B_\parallel \rangle_1}{40.3 \cdot f_1} + \frac{f_1^2}{40.3} \cdot \left(\lambda_1 N_1 + b^{GPS,L_1} + b_{LEO,L_1} + mp_{L_1} + \varepsilon_{L_1}\right), \tag{5}$$

$$STEC_2 = -\frac{(L_2 - \rho)}{40.3} \cdot f_2^2 - \frac{K \cdot \langle B_\parallel \rangle_2}{40.3 \cdot f_2} + \frac{f_2^2}{40.3} \cdot \left(\lambda_2 N_2 + b^{GPS,L_2} + b_{LEO,L_1} + mp_{L_2} + \varepsilon_{L_1}\right) \tag{6}$$

Thus, we estimate the STEC over both signal paths, and then form a STEC combination similar to that of the ionosphere-free linear combination:

$$STEC = \frac{STEC_1 \cdot f_1^2 - STEC_2 \cdot f_2^2}{f_1^2 - f_2^2} - \frac{K \cdot \overline{B_\parallel} \cdot (STEC_1 \cdot f_1 - STEC_2 \cdot f_2)}{40.3 \cdot \left(f_1^2 - f_2^2\right)} + \frac{1}{40.3 \cdot \left(f_1^2 - f_2^2\right)} \cdot \left[\left(\varepsilon_{L_1} f_1^4 - \varepsilon_{L_2} f_2^4\right) + \right.$$
$$\left. + \left(\lambda_1 N_1 f_1^4 - \lambda_2 N_2 f_2^4\right) + \left(b^{GPS,L_1} f_1^4 - b^{GPS,L_2} f_2^4\right) + \left(b_{LEO,L_1} f_1^4 - b_{LEO,L_2} f_2^4\right) + \left(mp_{L_1} f_1^4 - mp_{L_2} f_2^4\right) \right] \tag{7}$$

The third term in the brackets in the right-hand-side of Eq. (7) obtains small values, thus it can safely be omitted. To estimate the second-order ionospheric delay, ionosphere and geomagnetic field models are commonly used. Yet, the source of the second-order ionospheric delay in GPS measurements is the Faraday rotation effect that causes phase shift on GPS signals [*De Roo et al.,* 2004] and is proportional to the square of the wavelength, to the electron number density and to the Earth's magnetic field along the signal path. Hence, the second-order ionospheric delay can be expressed as:

$$s_1 = \frac{2\pi m^2 c^4 K \beta}{\lambda^2 e^3 f_1^3} \tag{8}$$

where β is the signal phase shift (radians), c is the speed of light in vacuum (m/s), e is the electron charge (C), m is the electron mass and K is a constant.

III. Model results and discussion

Figure 1*a* shows the L_1 and L_2 phase delays as function of time, ranging within [-7, -15] m for a setting RO event on 2 December 2006 at 19:27 h. The ionospheric RO event examined herein exhibits small fluctuations. These fluctuations are attributed to ionospheric variations, particularly when the GPS signals traverse the lower ionosphere, and to uncorrected receiver clock residual errors.

Figure 1*b* presents STEC values free from second-order ionospheric effects (our algorithm; black line) within [70, 110] TECU. Applying *Syndergaard* [2002] algorithm (red) on the same phase delays, we obtain values within [68, 108] TECU. The difference between the two algorithms is ~2.5 TECU (light blue line) and is primarily attributed to the second-order ionospheric term not accounted in *Syndergaard's* [2002] equation. The linear regression applied to the STEC obtained from our algorithm (black dashed line) shows that the STEC increase linearly with time, having a *y*-intercept of 68.4±0.82 TECU and a slope of 0.03±0.001 TECU/s.

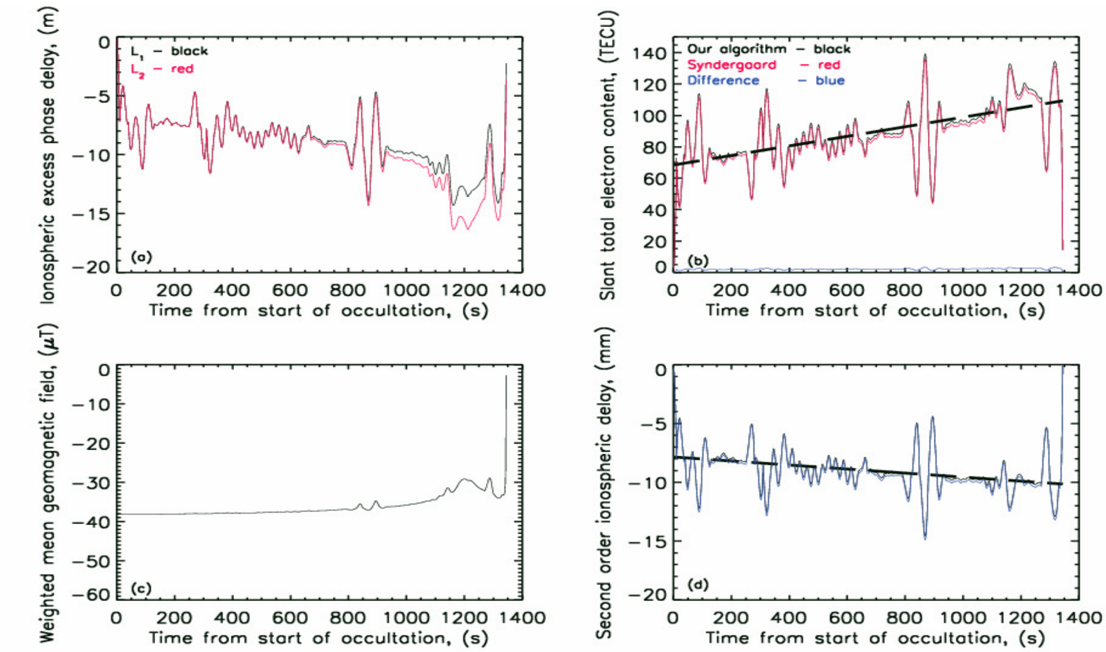

Figure 1: ***(a)*** *L_1 (black) and L_2 (red) ionospheric phase delays,* ***(b)*** *STEC retrieved from our (black) and Syndergaard's, [2002] (red) algorithms and their difference (blue),* ***(c)*** *weighted mean geomagnetic field values and* ***(d)*** *second-order ionospheric delays as function of occultation time computed using the Faraday rotation effect (Eq. 8; blue).*

Figure 1*c* illustrates weighted mean geomagnetic field values as function of time, computed as a by product of our research by dividing the results obtained from Eq. (8) with the STEC estimates from Fig. 1*b* (our algorithm; black line). The geomagnetic field obtains almost a constant value ranging within [-38, -35] μT, supporting the assumption made by *Kedar et al.* [2003] and *Hoque and Jakowski* [2007] of a constant geomagnetic field in their studies. The negative sign indicates the opposite direction of the geomagnetic field with respect to the GPS signal path.

Figure 1*d* demonstrates that the second-order ionospheric delay increases linearly as function of time obtaining values between [-8, -10] mm, as shown in the linear regression (dashed black line) with a *y*-intercept and a slope of –7.85±0.08 mm and $-1.71\cdot10^{-3}\pm1.09\cdot10^{-4}$ mm/s, respectively. Our results show that second-order ionospheric delays are larger for RO events than the second-order ionospheric delay estimates for ground-based measurements, due to traveling longer distance in the ionosphere.

IV. Conclusions

This study proposed a novel algorithm to retrieve STEC free from the second-order ionospheric effect and accounted for the ray path split between the L_1 and L_2 GPS signals due to ionospheric bending. We demonstrated that the second-order ionospheric delay can be estimated in near-real time using the Faraday rotation, instead of ionosphere and geomagnetic models. The ability to estimate accurately both the STEC and the second-order ionospheric delay in GPS measurements has wide-ranging implications in geophysical sciences, particularly in improving the accuracy of the GPS point positioning. Implementing our proposed techniques into the existing state-of-the-art GPS processing packages such as, BERNESE and GYPSY, we could potentially achieve millimetre accuracy in precise point positioning, which is currently required in numerous geophysical research such as, crustal deformation and plate tectonics motion.

References

Anthes, R. A., P. A. Bernhardt, Y. Chen, L. Cucurull, K. F. Dymond, D. Ector, S. B. Healy, S. –P. Ho, D. C. Hunt, Y. –H. Kuo, H. Liu, K. Manning, C. McCormick, T. K. Meehan, W. J. Randel, C. Rocken, W. S. Schreiner, S. V. Sokolovskiy, S. Syndergaard, D. C. Thompson, K. E. Trenberth, T.-K. Wee, N. L. Yen, and Z. Zeng (2008), The COSMIC/FORMOSAT-3 mission: Early results, *Bull. Am. Meteorol. Soc.*, 89, pp. 313 – 333

Bos, A. G. (2005), Kinematics of the southwestern U.S. deformation zone inferred from GPS motion data, *J. Geophys. Res.*, *110*, B08405

De Roo, R.D., A. W. England, and J. Munn, Circular polarization for L-band radiometric soil moisture retrieval, *Aerospace Conference, 2004. Proceedings. 2004 IEEE*, vol.2, pp. 1015-1023, March 2004

Guier, W. H., and G. C. Weiffenbach (1960), A Satellite Doppler Navigation System, *Proceedings of the IRE,* 48(4), pp. 507–516

Hoque, M. M., N. Jakowski, (2007), Higher order ionospheric effect in precise GNSS positioning, *J. Geod.,* 81, doi:10.1007/s00190-006-0106-0

Kedar, S., G. A. Hajj, B. D. Wilson, and M. B. Heflin, (2003), The effect of the second order GPS ionospheric correction on receiver positions, *Geophys. Res. Lett.,* 30(16), 1829, doi:10.1029/2003GL017639

Longair, M., (1992), High Energy Astrophysics, Vol. 1, 2nd Edition, 440 p. *Cambridge University Press,* New York

Morton, Y. T., Q. Zhou, and F. van Graas (2009), Assessment of second-order ionosphere error in GPS range observables using Arecibo incoherent scatter radar measurements, *Radio Sci.,* 44, doi:10.1029/2008RS003888

Syndergaard, S., (2002), A new algorithm for retrieving GPS radio occultation total electron content, *Geophys. Res. Lett.,* 29(16), 1808, doi:10.1029/2001GL014478